Laser-Scanning Imaging System for 3-D Profile Measurements of Human Eye Fundus

Koji KOBAYASHI and Toshimitsu ASAKURA*

Abstract

A laser-scanning imaging system has been developed for rapid 3-D measurements of the eye fundus. It employs defocused image information of two detection planes in a confocal optical arrangement of the scanning laser ophthalmoscope (SLO).

The 3-D fundus profiles which are difficult to obtain from the ordinary SLOs are obtainable by this system in vivo in real-time at the standard television rate. The 3-D imaging characteristics vary with wavelengths of laser beams used. The 3-D surface topography of the fundus is stably achieved by the wavelength of yellow light for many subjects without dilatation doses of the pupil.

1. Introduction

Three-dimensional (3-D) imaging and topographical measurements of the eye fundus are of great importance in ophthalmology. In recent years, scanning laser ophthalmoscopes (SLOs) have also exploited the possibilities for 3-D measurements by adopting confocal optical arrangements [1-3]. They record a tomographic series by shifting a confocal aperture placed at a detection plane that is conjugate to the subject's retina. In principle, the method is based on a coaxial use of the optical system in the eyeball structure. Therefore, it has the feasibility of better accuracy in comparison with other conventional techniques by the off-axial use of eye optics: stereoscopic photography or grid projection methods [4].

One of the problems in the SLO for the tomographic series exists in the difficulty of

Optics and Electronics Division, Kowa Company, Ltd.
1-3-1 Shinmiyakoda, Hamamatsu, Shizuoka 431-2103, Japan
* Faculty of Engineering, Hokkai-Gakuen University
Minami 26 Nishi 11, Chuo-ku, Sapporo, Hokkaido 064-0926, Japan

rapid operation, because of the longitudinal scanning. Eye motions easily influence the 3-D data acquisition during the examination. Other problems include the large amount of memory capacity for the image data and the complexity of signal processing. These problems become troublesome in the actual instrumentation.

To solve these problems, we have developed a new SLO system for 3-D measurements [5,6]. It employs a confocal optical arrangement with two pairs of apertures and detectors. Obtaining the ratio of the two signals eliminates the information of fundus reflectivity from output signals of the two detectors and the profile information is obtainable at an ordinary TV frame rate. In this paper, the design of the 3-D imaging system with a confocal SLO is reported and the experimental results are discussed in relation to both the wavelengths of laser light and the practical use of the instrument.

2. System for the 3-D imaging

The optical arrangement of the 3-D imaging system is schematically shown in Fig. 1. Details of the system were already given in the previous papers [5-8], but the major points of the system design are described in this section.

One of the features of the system is characterized by the use of an acousto-optic deflector (AOD) and a galvanometer scanner as the light deflectors. A combination of

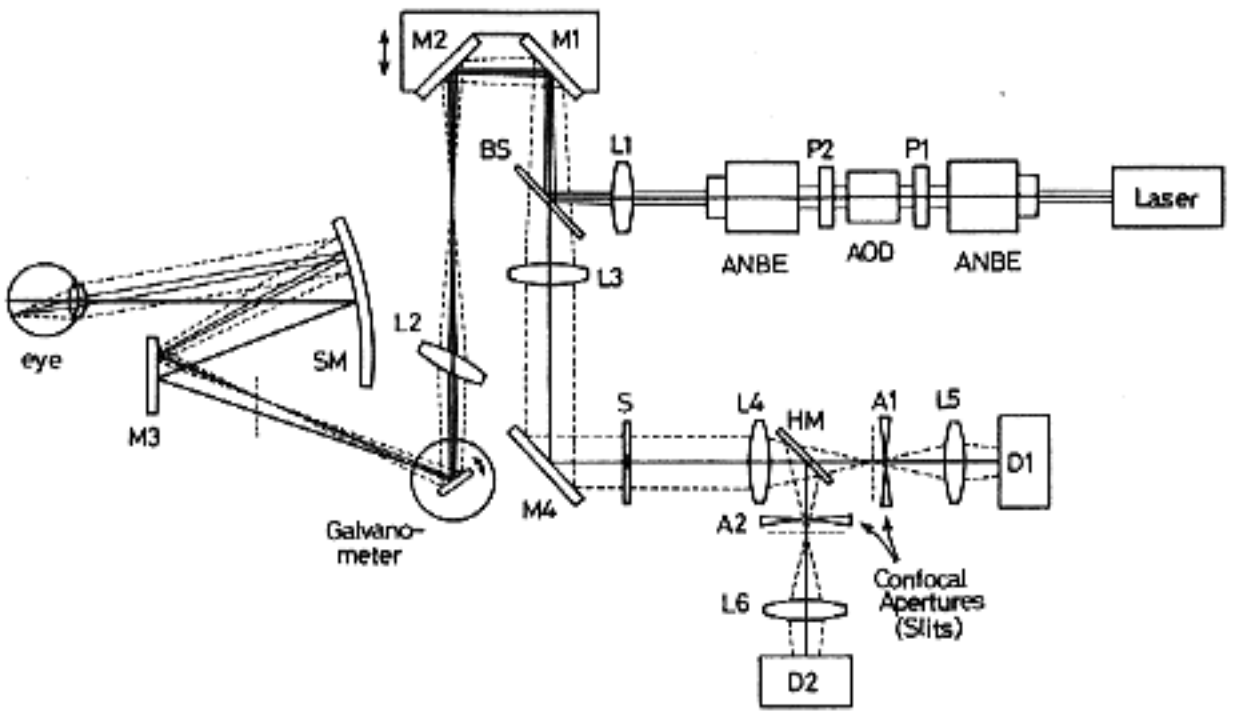

Fig. 1 Optical arrangement of the laser scanning system for the 3-D fundus imaging.

these deflectors enables the simple and easy control of synchronization in the scanning system. A laser beam from the laser light source (He-Ne laser: $\lambda = 632.8$nm, 594.1nm, or Ar laser: $\lambda = 514.5$nm, 488.0nm) is deflected by the AOD in a horizontal direction. The AOD is bracketed by anamorphic beam expanders (ANBEs) for beam shaping to an aperture of the acousto-optic crystal. The galvanometer scanner deflects the beam in a vertical direction which is perpendicular to the horizontal one by the AOD. The scanning frequencies of the two deflectors are 15.75kHz and 60Hz, respectively, corresponding to the ordinary TV system (NTSC standard). Two-dimensionally deflected laser rasters are projected into the subject's eye by an objective mirror (spherical mirror SM). A focusing mirror pair of M1 and M2 is provided to compensate any ametropia in the subject's eye.

In the whole system, the 3-D imaging function is performed by the light receiving section in the optical arrangement. The light from the eye fundus passes through a semitransparent beam splitter BS and a small light stop S that is provided to block the corneal reflex from the subject's eye. Passing through a lens L4 and a half-mirror HM, the light beam is focused near the two confocal apertures of A1 and A2. The apertures are composed of two parallel slits, which are displaced slightly from focal planes of the fundus along the optical axis. The light passing through the slits is detected by the two detectors of D1 and D2. We use silicon avalanche photodiodes (APDs) of high quantum efficiency as the light detectors. The imaging system with the APDs has a superior signal-to-noise ratio for the long-wavelength illuminations (a peak sensitivity at about 800nm) in the visible and infrared lights.

When the 3-D imaging is required with the above system, a focal plane of the fundus must be situated just between the two confocal apertures along the optical axis. This optical situation was adjusted by the focusing mirrors of M1 and M2 for ametropic subjects and confirmed by the signal level from the two detectors. Therefore, the light intensities detected by the detectors change in an opposite way according to height or depth conditions of the eye fundus: when the detected light intensity from one detector increases with the fundus unevenness, the light intensity from the other decreases.

Figure 2 explains the light intensity changes at the two detectors in this 3-D imaging system. In the figure, the curved lines of $f_1(z)$ and $f_2(z)$ indicate the functions by two confocal apertures and the peaks of each curve correspond to the positions of two slits of A1 and A2 in the optical configuration. Of course, the light intensity is dependent on the reflectivity of the eye fundus, which changes with the position of the scanning beam. In

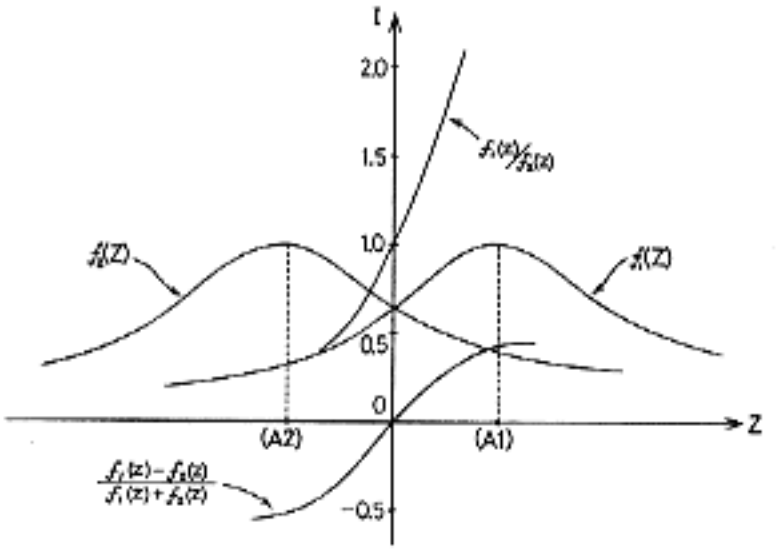

Fig. 2. Variation of the light intensities at the confocal apertures and the signal levels with respect to the ratio computations.

this system, therefore, the information of reflectivity was removed by division processings between the two detected signals. Two kinds of the function curves with respect to division calculations are shown in Fig.2 : $f_1(z)/f_2(z)$ or $\{f_1(z)-f_2(z)\}/\{f_1(z)+f_2(z)\}$, either of which can provide the 3-D topographic information by its signal level. In the actual instrument, these calculations are performed by an electronic video circuit with nonlinear gradation conversion and the results are displayed on a TV monitor in real-time. If the 3-D profile-data images have been precisely obtained, conversion of their original images into a sophisticated 3-D graphic representation is not very difficult with the use of digital image processors and computer softwares.

3. Results and discussion

In this imaging system, ordinary images are obtained from one detector channel (or from an added signal of two channels) by setting up the confocal aperture as well as the 3-D images from two detectors with two apertures. Figure 3 shows an example of the actual fundus images, all of which were obtained for the same subject's eye. In the figure, frame (a) shows an ordinary two-dimensional reflection image taken with a red He-Ne laser ($\lambda = 632.8$nm). The image represents the optic nerve head and its peripheral retinal vessels, and it also includes the information of choroidal tissues. On the other hand, frame (b) shows a reflection image of the same fundus taken with green light from an Ar laser ($\lambda = 514.5$nm). In the image of frame (b), the choroidal information has disappeared in

(a)

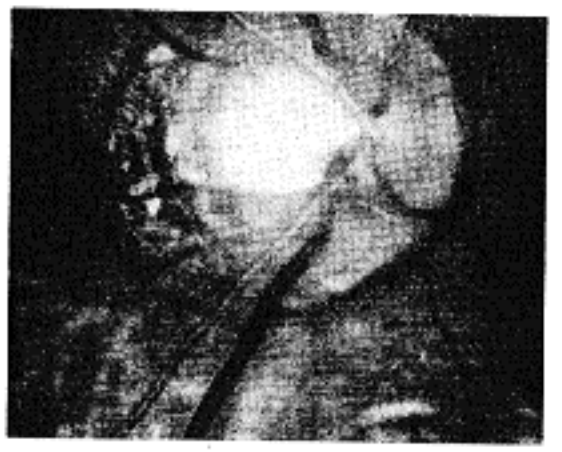

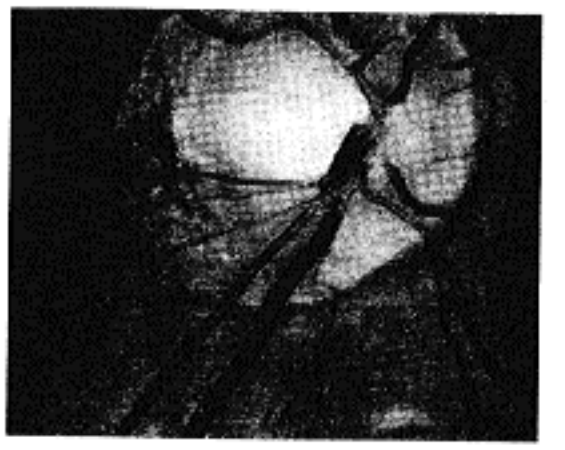

(b)

(c)

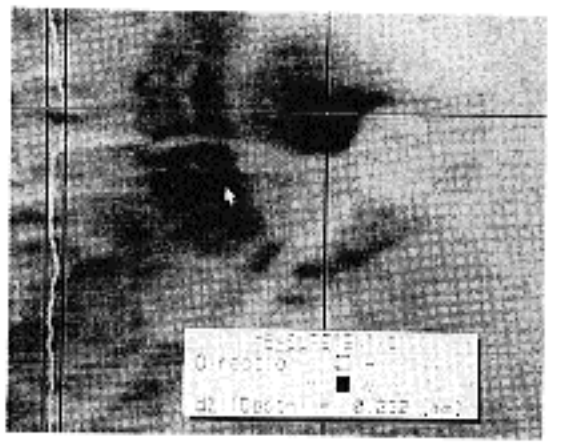

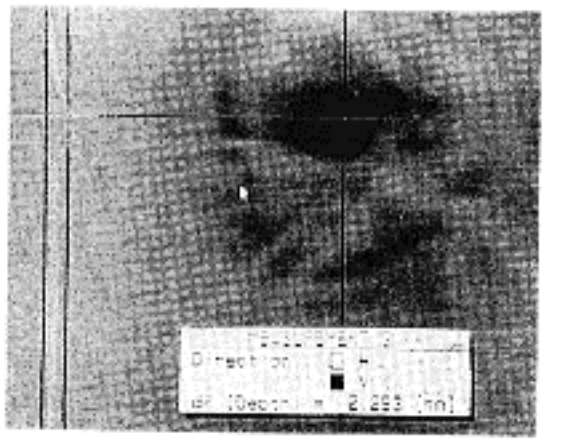

(d)

Fig. 3. Images of human subject's fundus: ordinary images (a) and (b), and 3-D topographic images (c) and (d). The frames (a) and (c) were taken with a red He-Ne laser ($\lambda = 632.8$nm), and (b) and (d) with a green Ar laser ($\lambda = 514.5$nm), respectively.

contrast with frame (a) taken with the red light.

Figure 3 (c) shows a 3-D profile data image by the ratio mode, which was taken with the red He-Ne laser. The image indicate the 3-D data Z(x,y) of the eye fundus, which is described as a black level for the deep portion, and a white level for the higher portion. The caved-in area in the optic nerve head, the upheaved thick vessels, and the influence of the choroidal tissue are also recognized. On the left side of the picture, a section profile on the vertical center line is indicated. On the other hand, Fig. 3 (d) shows a 3-D image of the same fundus taken with the green Ar laser. A section profile on the optic nerve head is also indicated at the left side of the picture, which shows that the influence of the choroidal tissue is little in the 3-D image by the green laser in comparison with the image taken with the red laser illumination.

The experimental results of the 3-D imaging under illumination of the red and green lights indicate the distinct differences in the 3-D fundus topography between the two wavelengths. The difference is considered to be due to the features of the several fundus

layers for the different colored light. In the ocular fundus, the red light passes through the retina and reaches the choroid. On the other hand, the green light is mainly reflected and scattered on the retinal tissues located in front of choroids [9,10]. Therefore, the 3-D images obtained by this imaging system are neither the simple results of inner limiting membrane nor the strict boundary between the vitreous and retina. The 3-D data detected by this system using the visual light illumination is the results of complicated phenomena due to the several fundus layers. In the vicinity of the optic papilla, the penetrating length of the laser beam through the tissue may vary with locations of the fundus.

Interesting imaging characteristics on the present system depend on the wavelengths of lasers used. The green or blue light illumination (λ =514.5nm or 488.0nm from Ar laser) may cause more specular reflections at the fundus in comparison with the longer wavelengths and these specular components deteriorate the 3D profile data images. In other words, the 3-D imaging principle of the system is based on diffuse reflection at the fundus tissue and the light intensity of any specular reflections hardly changes at the two confocal apertures. Several problems for the green and blue lights are the contraction of the ocular pupil under continuous illumination, the lower permissible exposure level, and the scattering within the eye media or the anterior segment.

Through experiments, we have empirically noticed that the yellow laser light is most appropriate for the stable observation of the 3-D fundus profiles in real-time. The yellow beam in the imaging system can detect the fundus contours distinctly in many subjects without dilatation doses of the pupil.

Figure 4 shows an example of fundus images of another subject's eye taken with a yellow He-Ne laser (λ =594.1nm). In the figure, frame (a) indicates an ordinary image by the regular confocal mode, which shows the optic nerve head with its peripheral retinal vessels in high contrast. When the yellow light is used, the arteries are observed more plainly than veins due to the extinction characteristic of oxyhemoglobin in blood vessels. On the other hand, frame (b) shows an image obtained by the ratio mode. In the image (b), the higher and deeper portions of the fundus are displayed in white and black levels, respectively. The subject has a physiological excavation in the optic nerve head of the eye fundus. Frames (c) and (d) show examples of the 3-D graphics converted from the image (b) by real-time computer signal processings. Frames (c) and (d) indicate the bird's-eye view representations from different sky angles, respectively. The fundus unevenness and excavation areas are intuitively recognizable from these 3-D graphic images.

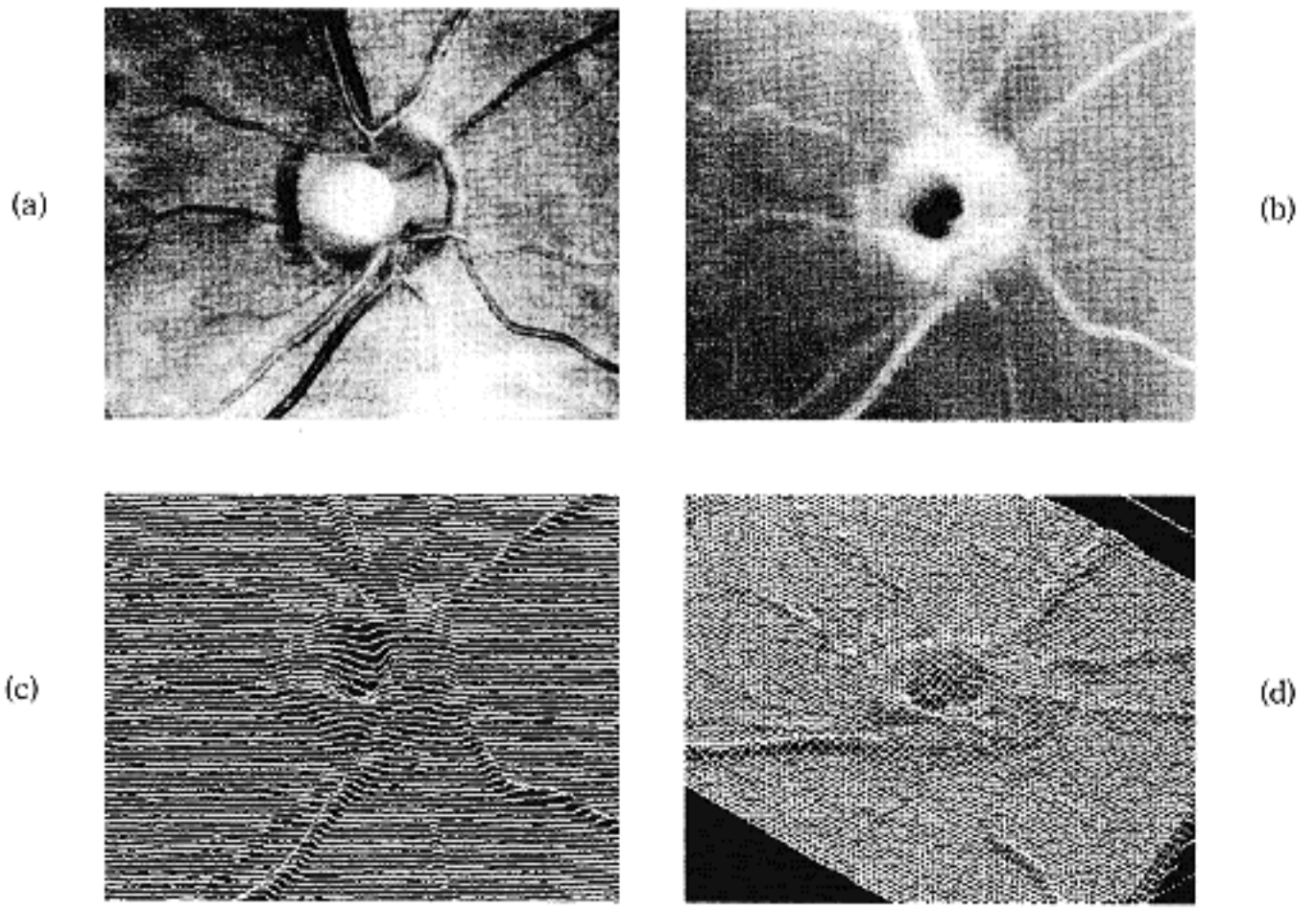

Fig. 4. Images of human-subject fundus taken with a yellow He-Ne laser (λ = 594.1nm): (a) the ordinary image, (b) the 3-D profile data image, (c) and (d) the 3-D graphic images, respectively.

In relation to the 3-D observations, optical coherence tomography (OCT) based on low-coherence light interferometry provides a better axial resolution in comparison with the confocal SLO [11,12]. However, the OCT has the difficulty of performing the rapid 3-D measurements and cannot produce ordinary reflection images in the scanning. The 3-D imaging function based on this laser scanning system offers novel outline survey techniques, which were difficult by the OCT and the other 3-D tomographic methods.

4. Conclusion

A laser-scanning imaging system for the 3-D measurements has been presented to provide a practical form in the SLO. The 3-D profiles of the eye fundus are successfully obtained in real-time from ratio computations of the two defocused images in a confocal optical arrangement. The 3-D images are influenced by each wavelength of the probing laser beam, which brings a variety of information from layered fundus tissues. To

confirm the effectiveness of the system in the medical use, clinical applications for the pathological fundus as well as for the normal subjects are required with actual instruments.

References

1. J. E. Wampler (ed), "New Methods in Microscopy and Low Light Imaging," SPIE Proc. **1161**: Sessions 7 and 8. (1989).
2. A. W. Dreher, J. F. Bille and R. N. Weinreb, "Active optical depth resolution improvement of the laser tomographic scanner," Appl. Opt. **28**: 804 (1989).
3. J. E. Nasemann and R. 0. W. Burk (ed.), "Scanning Laser Ophthalmoscopy and Tomography," Quint Essenz (1990).
4. B.R.Masters (ed.), "Noninvasive Diagnostic Techniques in Ophthalmology," Chapter 21, Springer-Verlag (1990).
5. K. Kobayashi, K. Akiyama, T. Suzuki, I. Yoshizawa and T. Asakura, "Laser-scanning imaging system for real-time measurelnents of 3-D objects profiles," Opt. Commun. **74**: 165 (1989).
6. K. Kobayashi, H. Matsui, H. Nakano and T. Asakura, "Real-time 3-D imaging of the fundus by scanning laser ophthalmoscopy," Opt.Commun. **87**: 9 (1992).
7. K. Kobayashi, H. Nakano, H. Matsui, K. Akiyama and T. Asakura, "Confocal scanning laser ophthalmoscope with a slit aperture," Meas. Sci. Technol. **2**: 287 (1991).
8. K. Kobayashi and T. Asakura, "Imaging techniques and applications of the scanning laser ophthalmoscope," Opt. Eng. **34**: 717 (1995).
9. F. C. Delori, E. S. Gragoudas, R. Francisco and R. C. Pruett, "Monochromatic ophthalmoscopy and fundus photography: the normal fundus," Arch. Ophthalmol. **95**: 861 (1977).
10. N. M. Ducrey, F. C. Delori and E. S. Gragoudas, "Monochromatic ophthalmoscopy and fundus photography: the pathological fundus," Arch. Ophthalmol. **97**: 288 (1979).
11. D. Huang, E. A. Swanson, C. P. Lin, J. S. Schuman, W. G. Stinson, W. Chang, M. R. Hee, T. Flotte, K. Gregory, C. A. Pliafito, and J. G. Fujimoto, "Optical coherence tomography," Science **254**, 1178 (1991).
12. A. Roorda and D. R. Williams, "New directions in imaging the retina," Opt. Photo. News 8, Feb. 23 (1997).